Available online at www.sciencedirect.com
ScienceDirect
International Journal of Thermal Sciences 47 (2008) 378–387
International Journal of Thermal Sciences
www.elsevier.com/locate/ijts

Numerical simulation of coupled heat transfers by conduction, natural convection and radiation in hollow structures heated from below or above

T. Ait-taleb, A. Abdelbaki *, Z. Zrikem

LMFE, Department of Physics, Cadi Ayyad University, Faculty of Sciences Semlalia, B.P. 2390, Marrakesh, Morocco

Received 7 June 2005; received in revised form 1 July 2006; accepted 22 January 2007

Available online 16 May 2007

Abstract

Coupled heat transfers in hollow structures uniformly heated from below or from above are numerically investigated. Discussions of the results are for structures formed by a range of 3 identical rectangular cavities with end vertical side walls of the structure assumed adiabatic or submitted to periodic conditions. The Boussinesq approximation is invoked and the flows are considered laminar and two-dimensional for the whole range of parameters considered. Conduction heat transfer in the solid partitions and surface radiation amongst grey diffuse surfaces are accounted for. The conservation equations are solved by a finite difference method and the pressure–velocity coupling solved by the SIMPLE algorithm.

Keywords: Hollow blocks; Horizontal structures; Heating from below; Heating from above; Conduction; Natural convection; Radiation; Overall thermal conductances; Numerical simulation

1. Introduction

Hollow structures are used in many practical applications such as building components, solar collectors, thermal energy storage systems, and so on. In general, the heat transfer in such structures is done simultaneously by conduction, natural convection and radiation. The coupling problems between the three modes of heat transfer have received last years a great attention. However, the available studies in the literature are generally limited to simple configurations consisting in rectangular cavities with one or several conducting walls. Earlier investigations were conducted by Balvanz and Kuehn [1] and Kim and Viskanta [2] on the interaction between the natural convection in a square cavity and the heat conduction in the adjacent walls. Effects of surface radiation on natural convection in a square enclosure filled with air were studied by Balaji and Venkateshan [3,4], Akiyama and Chong [5], Ramesh and Venkateshan [6] and Ramesh et al. [7]. In these studies, it has been shown that natural convection heat transfer is significantly reduced by conduction in the walls and/or radiation exchange between the cavity surfaces. Coupled heat transfers by conduction, natural convection and radiation in cellular structures with two vertical series of square cavities has been studied numerically by Abdelbaki and Zrikem [8]. Application was presented for building walls made of hollow clay tiles. Later, numerical solution of combined heat transfers in hollow clay tiles, with two air cells deep, submitted to transient thermal excitations was performed by Abdelbaki et al. [9]. Based on the simulation results the authors derived empirical transfer function coefficients for the hollow clay tiles by applying an identification technique.

However, in all works cited previously the studied structures were differentially heated by assuming the vertical sides isothermal while the horizontal ones are adiabatic. The problems where the hollow structures are heated from below are not well documented. Most of the available works studied the natural convection in rectangular cavities heated partially [10] or entirely [11–13] from below.

The aim of this paper is to study numerically the coupling between conduction, natural convection and surface radiation in horizontal hollow structures heated from below or above. These structures are formed by a series of rectangular cavities filled with air and having conducting partitions. The numerical

* Corresponding author. Tel.: +212 24 43 46 49 (post 489); fax: +212 24 43 74 10.
E-mail address: abdelbaki@ucam.ac.ma (A. Abdelbaki).

1290-0729/$ – see front matter
doi:10.1016/j.ijthermalsci.2007.01.035

Nomenclature

A	aspect ratio of the hollow structure, H/L
A_c	aspect ratio of the inner cavity, h/l
$\mathrm{d}F$	view factor between finite surfaces
$\mathrm{d}S$	finite area ..... m^2
E	incident radiative heat flux ..... $\mathrm{W\,m^{-2}}$
e_x	vertical partition thickness ..... m
e_y	horizontal partition thickness ..... m
G	temperature ratio, T_o/T_i
H	structure height ..... m
h	cavity height ..... m
J	radiosity ..... $\mathrm{W\,m^{-2}}$
J'	dimensionless radiosity, $J/(\sigma T_o^4)$
k	thermal conductivity ..... $\mathrm{W\,m^{-1}\,K^{-1}}$
L	structure depth ..... m
l	cavity width ..... m
N_k	thermal conductivity ratio, k_f/k_s
N_r	radiation to conduction number, $(\sigma T_o^4)H/k_s\Delta T$
Nu	Nusselt number
P	dimensionless pressure, $(p+\rho_0 gy)/\rho_0(\alpha_f/H)^2$
p	pressure ..... Pa
Pr	Prandtl number, ν/α_f
Q_a	dimensionless average heat flux
Q	average heat flux, $\frac{k_s\Delta T}{H}Q_a$ ..... $\mathrm{W\,m^{-2}}$
$q_{r,k}$	net radiative heat flux at surface k ..... $\mathrm{W\,m^{-2}}$
Q_{rk}	dimensionless net radiative heat flux at surface k, $q_{r,k}/\sigma T_o^4$
r	position on the cavity surface
r'	dimensionless position associated with r
Ra	Rayleigh number, $\frac{g\beta\Delta T H^3}{\nu\alpha_f}$
T	temperature ..... K
ΔT	temperature difference, (T_o-T_i) if $T_o>T_i$; (T_i-T_o) if $T_o<T_i$ ..... K
U, V	dimensionless velocity components in x and y directions, $(u,v)/(\alpha_f/H)$
X, Y	dimensionless Cartesian coordinates in x and y directions, $(x,y)/H$
X_c	position on the internal horizontal face of a cavity
Y_c	position on the internal vertical face of a cavity
Y_0	position in y direction of the lower horizontal side of a cavity

Greek symbols

α	thermal diffusivity ..... $\mathrm{m^2\,s^{-1}}$
β	thermal expansion coefficient ..... $\mathrm{K^{-1}}$
ε	cavity surface emissivity
η	dimensionless coordinate normal to a cavity surface
ν	kinematic viscosity ..... $\mathrm{m^2\,s^{-1}}$
ρ	fluid density ..... $\mathrm{kg\,m^{-3}}$
σ	Stephan–Boltzmann constant ..... $\mathrm{W\,m^{-2}\,K^{-4}}$
θ	dimensionless temperature, $(T-T_i)/\Delta T$
Ψ	dimensionless stream function
τ	dimensionless time, $t/(H^2/\alpha_f)$

Subscripts

a	above
b	below
conv	convection
f	fluid
i	inside
o	outside
rad	radiative
s	solid

code is tested by comparing its results with those reported in the literature for three different cases. Application results are presented for the hollow concrete blocks mostly used in the construction of building roofs using practical values of the thermal excitations. Overall thermal conductances are generated for the hollow concrete blocks for the two cases of heating (from below or above).

2. Mathematical formulation

2.1. Studied configuration and governing equations

The studied configuration, sketched in Fig. 1, is formed by a range of N_x rectangular cavities of width l and height h surrounded by solid partitions. The top and bottom sides of the hollow structure are considered isothermal and are maintained at temperatures T_o and T_i respectively. The structure vertical sides are considered adiabatic or submitted to periodicity conditions. In formulating governing equations, the problem is considered laminar and two-dimensional. The solid and fluid properties are assumed to be constant except for the density in the buoyancy term where the Boussinesq approximation is utilized. Viscous heat dissipation in the fluid is neglected. The fluid is assumed to be non-participating to radiation and the cavities inside surfaces are considered diffuse-grey. The governing equations are written in dimensionless form as:

$$\frac{\partial U}{\partial X}+\frac{\partial V}{\partial Y}=0 \tag{1}$$

$$\frac{\partial U}{\partial \tau}+U\frac{\partial U}{\partial X}+V\frac{\partial U}{\partial Y}=-\frac{\partial P}{\partial X}+Pr\left(\frac{\partial^2 U}{\partial X^2}+\frac{\partial^2 U}{\partial Y^2}\right) \tag{2}$$

$$\frac{\partial V}{\partial \tau}+U\frac{\partial V}{\partial X}+V\frac{\partial V}{\partial Y} =-\frac{\partial P}{\partial Y}+Pr\left(\frac{\partial^2 V}{\partial X^2}+\frac{\partial^2 V}{\partial Y^2}\right)+Ra\,Pr\,\theta_f \tag{3}$$

$$\frac{\partial \theta_f}{\partial \tau}+U\frac{\partial \theta_f}{\partial X}+V\frac{\partial \theta_f}{\partial Y}=\frac{\partial^2 \theta_f}{\partial X^2}+\frac{\partial^2 \theta_f}{\partial Y^2} \tag{4}$$

where U and V are the dimensionless velocity components in X and Y directions respectively, P is the pressure, θ_f is the fluid

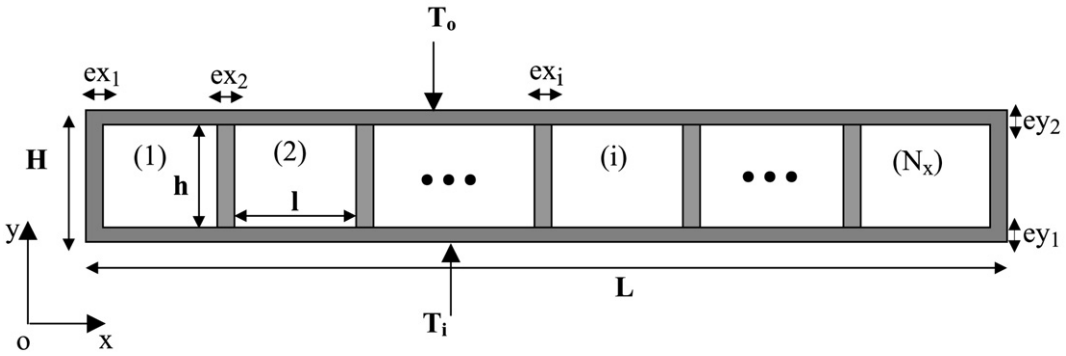

Fig. 1. Schematic diagram of the studied hollow structure.

temperature, Pr is the Prandtl number and Ra is the Rayleigh number given by:

$$Ra = \frac{g\beta H^3 \Delta T}{\nu^2} Pr$$

The dimensionless equation of heat conduction in the solid walls is:

$$\frac{\alpha_f}{\alpha_s}\frac{\partial \theta_s}{\partial \tau} = \frac{\partial^2 \theta_s}{\partial X^2} + \frac{\partial^2 \theta_s}{\partial Y^2} \tag{5}$$

where α_f and α_s are the fluid and the solid thermal diffusivities respectively and θ_s is the dimensionless solid temperature. The boundary conditions of the problem are:

- $U = V = 0$ on the inner sides of each cavity
- $\begin{cases} \theta_s(X,0) = 1 \text{ and } \theta_s(X,1) = 0 \quad (0 \leqslant X \leqslant L/H) \\ \text{for the heating from below case} \\ \theta_s(X,0) = 0 \text{ and } \theta_s(X,1) = 1 \quad (0 \leqslant X \leqslant L/H) \\ \text{for the heating from above case} \end{cases}$
- $\begin{cases} \theta_s(0,Y) = \theta_s(L/H,Y) \quad (0 \leqslant Y \leqslant 1) \\ \text{for the periodicity condition} \\ \frac{\partial \theta_s}{\partial X}\big|_{X=0;L/H} = 0 \quad (0 \leqslant Y \leqslant 1) \\ \text{for the adiabaticity condition} \end{cases}$

The continuity of the temperature and the heat flux at the fluid–wall interfaces gives:

$$\theta_s(X,Y) = \theta_f(X,Y) \tag{6}$$

$$-\frac{\partial \theta_s}{\partial \eta} = -N_k \frac{\partial \theta_f}{\partial \eta} + N_r Qr \tag{7}$$

where η represents the dimensionless coordinate normal to the wall, N_k is the thermal conductivity ratio k_f/k_s, Q_r is the dimensionless radiative heat flux and N_r is the dimensionless radiation to conduction parameter defined by:

$$N_r = \frac{\sigma T_o^4 H}{k_s \Delta T}$$

The dimensionless radiative heat flux Q_r is related to the radiative heat flux q_r by:

$$Q_r = \frac{q_r}{\sigma T_o^4}$$

The net radiative heat flux $q_{r,k}(r_k)$ exchanged by the finite area $\mathrm{d}S_k$, located at a position r_k on the surface k, is given by:

$$q_{r,k}(r_k) = J_k(r_k) - E_k(r_k) \tag{8}$$

where $J_k(r_k)$ is the radiosity and $E_k(r_k)$ is the incident radiative heat flux on the surface $\mathrm{d}S_k$ given respectively by:

$$J_k(r_k) = \varepsilon_k \sigma \left(T_k(r_k)\right)^4 + (1-\varepsilon_k) E_k(r_k) \tag{9}$$

$$E_k(r_k) = \sum_{j=1}^{4} \int_{A_j} J_j(r_j)\, \mathrm{d}F_{\mathrm{d}S_k - \mathrm{d}S_j(r_k, r_j)} \tag{10}$$

where ε_k is the emissivity of the surface k and $\mathrm{d}F_{\mathrm{d}S_k - \mathrm{d}S_j}$ is the view factor between the finite surfaces $\mathrm{d}S_k$ and $\mathrm{d}S_j$ located at r_k and r_j respectively. Taking into account Eqs. (8) to (10), the dimensionless radiative heat flux can be expressed as:

$$Q_{r,k}(r'_k) = \varepsilon_k \left(\left| 1 - \frac{1}{G} \right| \theta_k(r'_k) + \frac{1}{G} \right)^4 - \varepsilon_k \sum_{j=1}^{4} \int_{S_j} J'_j(r'_j)\, \mathrm{d}F_{\mathrm{d}S_k - \mathrm{d}S_j} \tag{11}$$

where G is the temperature ratio T_o/T_i, $J'_j(r_j)$ is the dimensionless radiosity at the position r_j on surface j. By dividing the walls into finite isothermal surfaces, Eq. (11) leads to a set of linear equation where the unknowns are the dimensionless radiosities $J'_j(r_j)$.

The dimensionless average heat flux across the structure is given by:

$$Q_a = -\frac{H}{L} \int_0^{\frac{L}{H}} \frac{\partial \theta_s}{\partial Y}\bigg|_{Y=0} \mathrm{d}X = -\frac{H}{L} \int_0^{\frac{L}{H}} \frac{\partial \theta_s}{\partial Y}\bigg|_{Y=1} \mathrm{d}X \tag{12}$$

To evaluate the rate of convective heat transfer on the internal horizontal surface of a cavity, the average Nusselt number is given by:

$$Nu = -\frac{H}{l} \int_0^{\frac{l}{H}} \left(\frac{\partial \theta_f}{\partial Y} \right)_{Y=Y_0} \mathrm{d}X \tag{13}$$

The dimensionless convective heat flux received by the fluid is given by:

$Q_{\text{conv}} = Nu$ for $Y = Y_0$ and
$Q_{\text{conv}} = -Nu$ for $Y = (l/L - Y_0)$

2.2. Method of solution and parameters of simulation

Governing equations are discretised using the finites differences method based on the control volumes approach with a power law scheme and are solved by the SIMPLE algorithm. The resulting system of algebraic equations is solved by the Tri-Diagonal-Matrix-Algorithm. To accelerate the convergence of solutions, the governing equations are solved in their instationary form.

2.2.1. Validation of the calculation code

The numerical code has been validated by comparing its results with those reported in the literature in the two following different cases:

(i) Interaction between natural convection and radiation in a square cavity. The average convective and radiative Nusselt numbers calculated at the hot surface of the enclosure for different values of the emissivity ε and for $10^3 \leqslant Ra \leqslant 10^6$ are compared in Figs. 2 and 3 with those obtained by Akiyama and Chong [5] and by Balaji and Venkateshan [4]. As shown there is a good agreement between the different results.

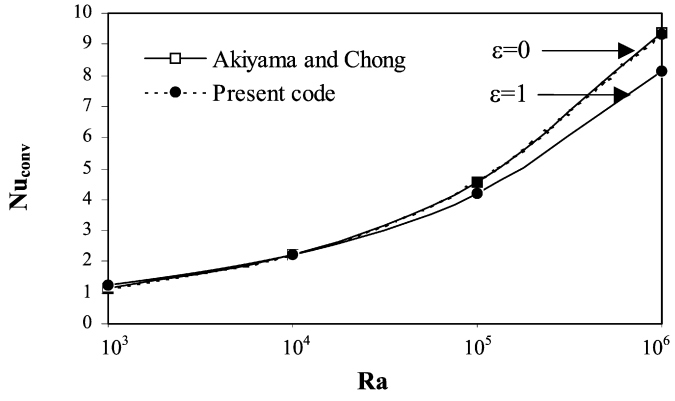

Fig. 2. Variations of the average Nusselt convection number as a function of Ra for $\varepsilon = 0$ and $\varepsilon = 1$.

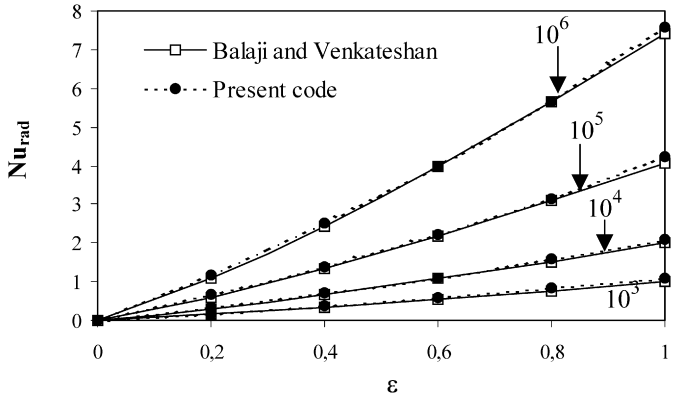

Fig. 3. Variations of the average Nusselt radiation number as a function of ε for different values of Ra.

(ii) Natural convection in a heated from below square cavity. Results given in Table 1 show that the Nusselt number and the maximum stream function obtained for different Rayleigh numbers in the present study are in good agreement with those predicted in the works of Lakhal and Hasnaoui [11], Strada and Heinrich [12] and Hamady et al. [13].

2.2.2. Parameters of the simulation

The numerical procedure presented in this paper is applied to predict heat exchanges through the hollow concrete blocks used in practice to construct building roofs. Results are presented for the three types of hollow block mostly used in Morocco, whose geometrical parameters are given in Table 2. Each hollow block is formed by three rectangular cells surrounded by concrete partitions. The hollow block considered differ by the aspect ratio of the internal cavities A_c which is a main geometrical parameter because it influences significantly the heat exchange and the fluid motion in the cavities. To realize a compromise between accuracy and computation time, a study on the effects of both grid spacing and time step on the simulation results has been conducted for each type of hollow blocks. This study leads to the uniform grid given in Table 3. The dimensionless time used in the simulation is 10^{-5}. The convergence criterion is based

Table 1
Comparison of results of the present work with those of Lakhal and Hasnaoui [11], Strada and Heinrich [12] and Hamady et al. [13] in the case of a square cell heated from below

Ra	Strada and Heinrich (1982)	Lakhal and Hasnaoui (1994)	Hamady et al. (1989)	Present code
10^4	$Nu = 2.153$	–	–	$Nu = 2.164$
1.5×10^4	–	–	$Nu = 2.34$	$Nu = 2.321$
5.6×10^4	–	–	$Nu = 3.78$	$Nu = 3.675$
10^5	$Nu = 3.888$	$Nu = 4.00$	$Nu = 4.01$	$Nu = 3.917$
	–	$\Psi_{\max} = 25.9$	–	$\Psi_{\max} = 25.1$
1.1×10^5	–	–	$Nu = 4.50$	$Nu = 4.282$
2.1×10^5	–	–	$Nu = 5.60$	$Nu = 5.512$
10^6	–	$Nu = 6.91$	–	$Nu = 6.702$
	–	$\Psi_{\max} = 75.0$	–	$\Psi_{\max} = 73.2$

Table 2
Dimensions of the studied hollow blocks

Aspect ratio	l (m)	h (m)	e_x (m)	e_y (m)	$A_c = h/l$
$A_c = A_{c1} \approx 1/4$	0.13	0.035	0.025	0.02	0.26
$A_c = A_{c2} \approx 1/2$	0.13	0.07	0.025	0.02	0.53
$A_c = A_{c3} \approx 1$	0.13	0.1	0.025	0.02	0.77

Table 3
Adopted grids for each studied type of hollow block

Aspect ratio	Grid	Grid in each cavity
$A_c = A_{c1} \approx 1/4$	80×20	17×17
$A_c = A_{c2} \approx 1/2$	80×30	17×27
$A_c = A_{c3} \approx 1$	80×40	17×37

on the relative change in the variables U, V, P, θ and Q_r at different nodes of the calculation domain:

$$\left|\frac{f^{n+1}(i,j) - f^{n}(i,j)}{f^{n}(i,j)}\right| \leqslant 10^{-4}$$

where $f^n(i,j)$ is the variable f ($f = U, V, P, \theta, Q_r$) value at node (i,j) calculated at iteration n.

3. Results and discussions

Generally, in practical situations such as that studied here, the geometrical parameters of the system under investigation are fixed. Therefore, the thermal behavior of this system is function only of the thermal excitations (T_o and T_i). Furthermore, it is recognized that in problems where the natural convection is coupled to the radiation, the heat transfer rate does not depend only on the temperature difference ΔT but depends of the values of T_o and T_i (or T_i and ΔT). For these reasons, the governing parameters that will be used in the present analysis are T_o and T_i instead of Ra and N_r.

The hollow blocks considered are in light concrete, characterized by a thermal conductivity $k_s = 0.5\ \mathrm{W\,m^{-1}\,K^{-1}}$ and emissivity $\varepsilon = 0.9$. The air thermal conductivity k_f and diffusivity α_f are equal to $0.0262\ \mathrm{W\,m^{-1}\,K^{-1}}$ and $1.57 \times 10^{-5}\ \mathrm{m^2\,s^{-1}}$ respectively. The Prandtl number is $Pr = 0.71$. The Rayleigh number (Ra) and the radiation to conduction number (N_r) are functions of the temperatures T_o and T_i. Results are presented for $T_i = 20\,^\circ\mathrm{C}$ and $1\,^\circ\mathrm{C} \leqslant \Delta T \leqslant 30\,^\circ\mathrm{C}$: $T_o = T_i - \Delta T$ for the heating from below case and $T_o = T_i + \Delta T$ for the heating from above case. This range covers the temperature differences that occur in practice and it corresponds to $3.97 \times 10^4 \leqslant Ra_H \leqslant 7.75 \times 10^6$ and $2.089 \leqslant N_r \leqslant 117.006$.

3.1. Hollow blocks heated from below

3.1.1. Streamlines and isotherms

3.1.1.1. Effect of the temperature difference ΔT. Figs. 4(a)–4(c) show the streamlines contours (at the top) and the isotherms (at the bottom) obtained for $\Delta T = (T_i - T_o) = 5\,^\circ\mathrm{C}$, $15\,^\circ\mathrm{C}$ and $30\,^\circ\mathrm{C}$ respectively. It can be seen that, the flow structures in each hollow block are characterized by two adjacent cells circulating in opposite directions and which are not perfectly symmetrical. As expected, the size of the central cell increases slightly when ΔT increases (from (a) to (c)) indicating a flow intensity increase. In fact, the values of the maximum stream function $\Psi_{\max}$ for the central streamline are 11.43 for $\Delta T = 5\,^\circ\mathrm{C}$, 43.59 for $\Delta T = 15\,^\circ\mathrm{C}$ and 60.28 for $\Delta T = 30\,^\circ\mathrm{C}$.

Concerning the temperature field, the isotherms distortion in the cavities is due to the natural convection heat transfer. In the solid walls separating the cavities the temperature profile is almost linear for $\Delta T = 5\,^\circ\mathrm{C}$ (Fig. 4(a)). This linear character is violated progressively when ΔT increases (Figs. 4(b) and (c)). The concentration of the isotherms near the horizontal surfaces of the cavities indicates an important gradient of temperature in these regions due to the great difference between the solid and the fluid conductivities ($N_k = 0.0524$).

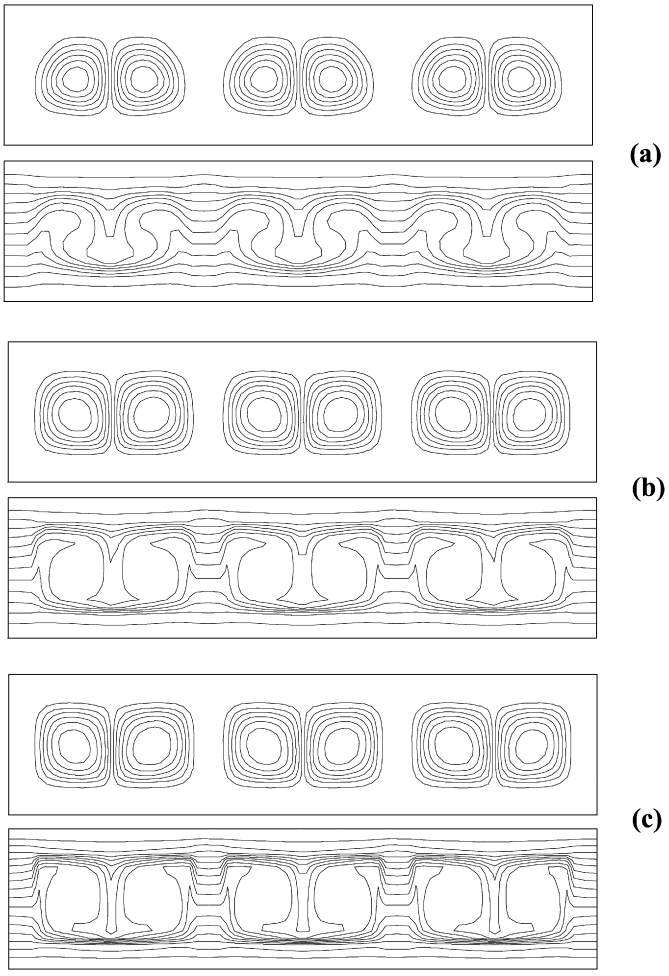

Fig. 4. Streamlines and isotherms obtained in heating from below for $A_c = A_{c2}$ and: (a) $\Delta T = 5\,^\circ\mathrm{C}$; (b) $\Delta T = 15\,^\circ\mathrm{C}$; (c) $\Delta T = 30\,^\circ\mathrm{C}$.

3.1.1.2. Effect of the aspect ratio of internal cavities A_c. For $\Delta T = 20\,^\circ\mathrm{C}$, Figs. 5(a)–(c) present the streamlines and the isotherms obtained respectively for $A_c = A_{c1}$, $A_c = A_{c2}$ and $A_c = A_{c3}$. Examination of the flow structures obtained for each value of A_c, shows that the number n of cells in each cavity is almost equal to the inverse of the aspect ratio of this cavity ($n \approx 1/A_c$). In fact, for a small aspect ratio ($A_c \approx 1/4$) the flow is characterized by four small cells ($n = 4$) of low intensity ($\Psi_{\max} = 16.2$). When the aspect ratio increases the number of cells decreases. Then, for ($A_c \approx 1/2$) the flow is characterized by tow symmetrical cells ($n = 2$) with a moderate intensity ($\Psi_{\max} = 43.59$) while for a great aspect ratio ($A_c \approx 1$) the flow is more intensive ($\Psi_{\max} = 82.03$) and is characterized by a single cell ($n = 1$). The flow intensity increase is due to the natural convection which finds more space to be developed. The narrowing of isotherms at the bottom of the cavity in each case indicates a good heat transfer near the active walls. Results obtained for $A_c \approx 1/4$ and $A_c \approx 1/2$ show that the central vertical axis of the hollow block is a symmetry axis for both flow and heat transfer. This result can be used to reduce the calculation domain to the half of the system. This permits significant reduction of the computational time.

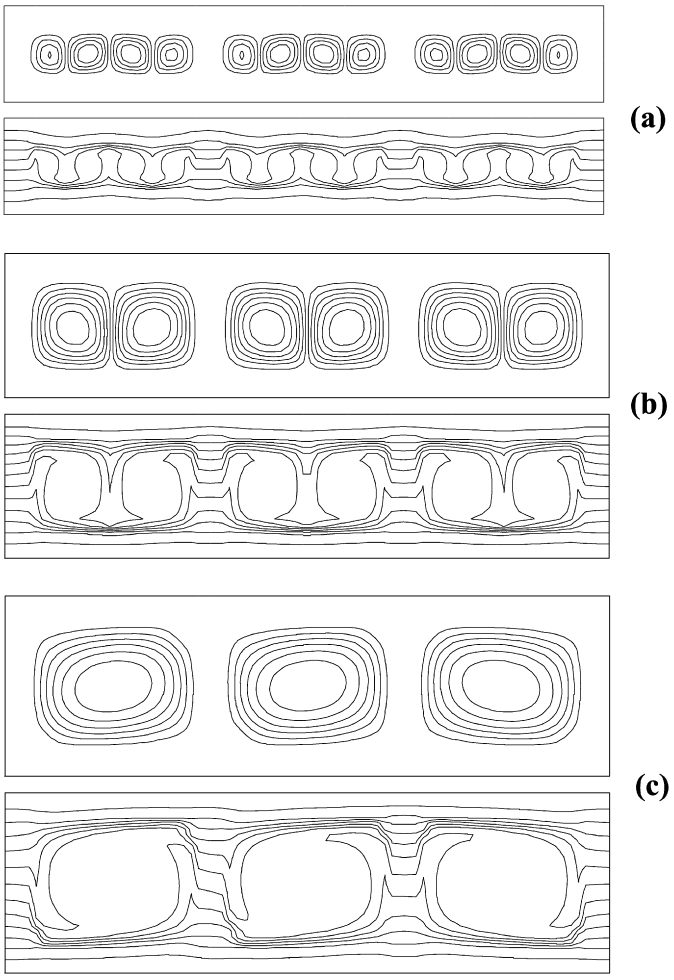

Fig. 5. Streamlines and isotherms obtained in heating from below for $\Delta T = 20\,^{\circ}\mathrm{C}$ and different aspect ratios: (a) $A_c = A_{c1}$; (b) $A_c = A_{c2}$; (c) $A_c = A_{c3}$.

3.1.2. Effect of the boundary conditions imposed on the vertical walls

Tests on both flow and heat transfer were made on the influence of the periodicity or the adiabaticity conditions imposed on the system vertical limits. These tests showed that the flow nature and the temperature distribution obtained for the two conditions are similar. Concerning the heat flow, Fig. 6 shows the variations of the mean vertical heat flux Q ($\mathrm{W\,m^{-2}}$) through the system as a function of the temperature difference ΔT (°C) between the horizontal surfaces. As shown, there is an excellent agreement between the results obtained by applying the two boundary conditions. In fact, the differences observed are lower than 0.4%. However, it has been recorded that the periodicity condition permits fast convergence of the numerical solution. It should be noted that the overall heat transfer through the system varies almost linearly with the temperature difference ΔT between the top and bottom surfaces. This is mainly due to the dominance of the conduction heat transfer which represents 59.3% from the overall heat transfer for $\Delta T = 10\,^{\circ}\mathrm{C}$, 56.1% for $\Delta T = 20\,^{\circ}\mathrm{C}$ and 51.8% for $\Delta T = 30\,^{\circ}\mathrm{C}$.

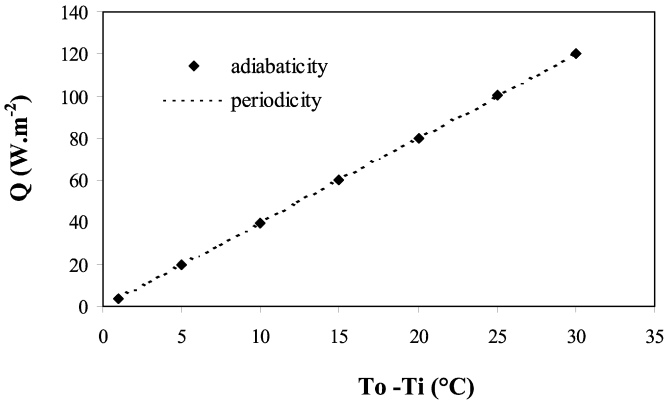

Fig. 6. The effect of adiabaticity and periodicity conditions on the global heat flow.

3.1.3. Heat transfer by radiation

The results presented in this part have been carried out for the case $A_c \approx 1/2$, $\Delta T = 30\,^{\circ}\mathrm{C}$ and $T_i = 20\,^{\circ}\mathrm{C}$. For the three cavities of the block, Fig. 7 gives the distributions of the dimensionless radiative heat flux Q_r exchanged by the horizontal surfaces (Fig. 7(a)), the vertical left surface (Fig. 7(b)) and the vertical right one (Fig. 7(c)). Theses figures give the variation of Q_r as a function of the positions X_c and Y_c counted from the left lower corner of the cavity. It can be seen that the heat flux received by the upper horizontal surface (cold surface) reaches its maximum near the middle of the surface ($X_c = 0.125$) and decreases toward the corners. However, for the lower horizontal surface (hot surface), a slight diminution of the radiative heat transfer is observed near the middle of the surface. This diminution can be explained by the attenuation of the radiation by the natural convection which is maximum at this level (see Fig. 8(a)). This phenomenon which will be discussed in detail in Section 3.1.4. is not appreciable on the upper horizontal surface of the cavity. The radiative heat transfer distributions in the three cavities of the hollow structure are similar. The difference observed between radiative heat fluxes in the cavities (1) and (3) on one hand and the cavity (2) on the other hand is negligible and is due to the edge effects resulting from the adiabaticity conditions that are imposed on the vertical sides of the structure.

Concerning the radiative behavior of the vertical sides, Figs. 7(b) and (c) show that, as expected, the lower parts of theses sides lose the heat by radiation while the upper parts receive it with a practically void radiative heat flux in the central regions. However, the rate of heat exchanged by radiation at the vertical surfaces is very weak compared to that exchanged by the horizontal sides.

3.1.4. Convection heat transfer

Since each cavity has four conducting walls, it is more interesting to evaluate the dimensionless convective heat flux received by the fluid (Q_{conv}) on each one of these walls. For $A_c \approx 1/2$, $\Delta T = 30\,^{\circ}\mathrm{C}$ and $T_i = 20\,^{\circ}\mathrm{C}$ Fig. 8 gives the variation of Q_{conv} along the horizontal and vertical faces of the cavities (1)–(3). For the lower horizontal face of each cavity (Fig. 8(a)), Q_{conv} reaches its maximum value near the middle

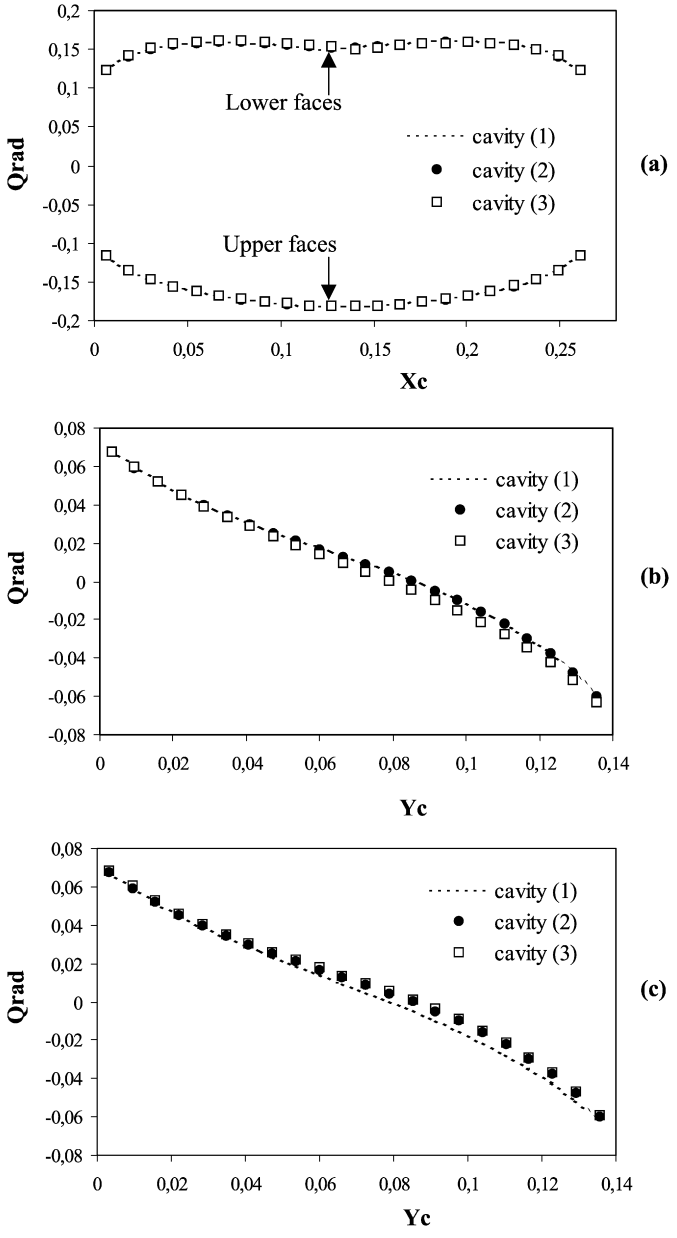

Fig. 7. Variations of the dimensionless radiative heat flux on the internal cavities surfaces: (a) horizontal faces; (b) left vertical faces; (c) right vertical faces.

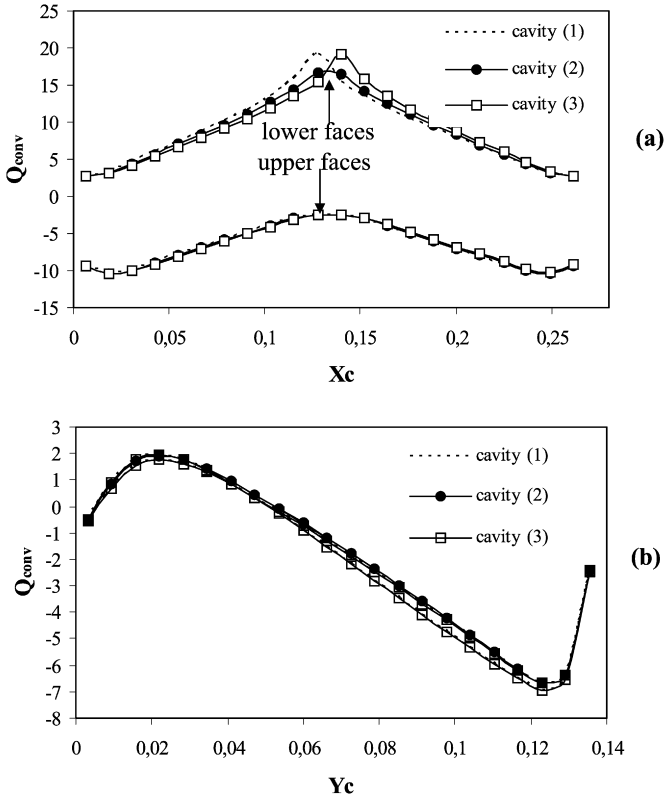

Fig. 8. Variations of dimensionless convective heat flux along the: (a) horizontal faces; (b) vertical faces.

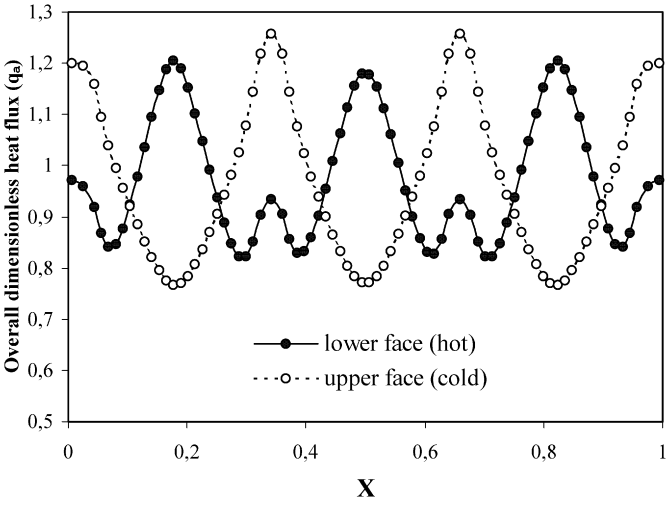

Fig. 9. Variations of the overall dimensionless heat flux through the structure as a function of X for $A_c = A_{c2}$ and $\Delta T = 30\,^{\circ}\mathrm{C}$.

of the surface ($X_c = 0.125$) where the temperature gradient is very intense. This have been shown clearly in the temperature distribution given in Fig. 4 which shows significant fall of temperature at the level of the central vertical axis of the cavity. This fall of temperature is due to the movement of the fluid going down after having released the heat which transported to the upper parts of the cavity. For the upper horizontal surfaces, the maximum of convective heat transfer is always at the level of the central parts but the variation of the Q_{conv} with X_c is relatively moderate. It should be noted that for the lower horizontal surfaces there are appreciable differences near the maximum between the results obtained for the cavities (1)–(3). These differences can be justified by the edge effects mentioned previously in Section 3.1.3. The results obtained for the vertical surfaces (Fig. 8(b)) show that the fluid heated by the lower horizontal wall continues to receive heat from the lower parts of the vertical walls, which are heated by conduction, and begins to restore the heat at the higher parts of the solid matrix of the structure. However, the convective heat transfer on the vertical surfaces remains very lower than that on the horizontal surfaces.

3.1.5. *Overall heat transfer in the vertical direction*

Fig. 9 obtained for $T_i = 20\,^{\circ}\mathrm{C}$, $\Delta T = 30\,^{\circ}\mathrm{C}$ and $A_c = A_{c2} \approx 1/2$ gives the distribution of the local dimensionless heat flux

($q_a = (-\frac{\partial \theta_s}{\partial Y})_{Y=0,1}$) crossing the lower face ($Y = 0$) of the block and the upper one ($Y = 1$) as a function of the position X. As expected, the heat transfer through the lower surface is more significant opposite to the cavities and is maximum in front of the centers of cavities. This can be explained by the significant temperature gradient between the hot solid wall and the cold fluid that comes down along the vertical axis of the cavity (see Figs. 4 and 5). The heat flow decreases towards the corners of the cavities. Also, the heat flux through the lower face presents small peaks at the center of the vertical solid walls, which are due essentially to the conduction heat transfer in the vertical direction. These small peaks indicate that the conductive heat transfer through a vertical solid partition separating too adjacent cavities is limited by the fact that the fluids circulating on both sides of this wall tend to homogenize the temperature in the upper part of the partition. For the upper horizontal side of the structure, the situation observed above (for the lower side) is reversed and the heat flux is maximum at the medium of the vertical partitions heated by both conduction and convection and reaches its minimal value at the level of the central vertical axis of the cavity where the temperature gradient is extremely weak.

3.2. Heating from above

In practice, the temperature of the upper surface of the block can be inferior or superior to that of the lower surface. This justifies the other situation where the hollow block is heated from above. For $\Delta T = (T_o - T_i) = 15\,^{\circ}\mathrm{C}$ and $T_i = 20\,^{\circ}\mathrm{C}$, Fig. 10 illustrates the streamlines and the isotherms obtained for the three types of hollow blocks. As expected, the analysis of the temperature field shows that the heat transfer in each medium (solid wall or air) is almost linear and is done mainly by conduction and radiation. The small distortions of the isotherms are due to the difference between the conductivities of the solid and the fluid. Concerning the streamlines (Fig. 10(a)), the small cells which appear in each cavity are due to a fluid flow of low intensity resulting from the variation in temperature created by conduction and radiation in the corners of the cavities. The nature of the flow and the temperature distribution are not significantly affected by the aspect ratio because of the absence of convection heat transfer.

3.3. Global heat transfer

To study the variation of the overall heat transfer across the structure as a function of the temperature difference ΔT, it is useful to calculate the contribution of each heat transfer process in the overall heat flux Q. Then, at $Y = Y_0$, dimensionless heat fluxes by conduction (Q_{cond}), convection (Q_{conv}) and radiation (Q_{rad}) are given respectively by:

$$Q_{\mathrm{cond}} = -\frac{H}{ex_1}\int_0^{\frac{ex_1}{H}} \left.\frac{\partial \theta_s}{\partial Y}\right|_{Y=Y_0} \mathrm{d}X - \frac{H}{ex_2}\int_{\frac{ex_1+l}{H}}^{\frac{ex_1+ex_2+l}{H}} \left.\frac{\partial \theta_s}{\partial Y}\right|_{Y=Y_0} \mathrm{d}X$$

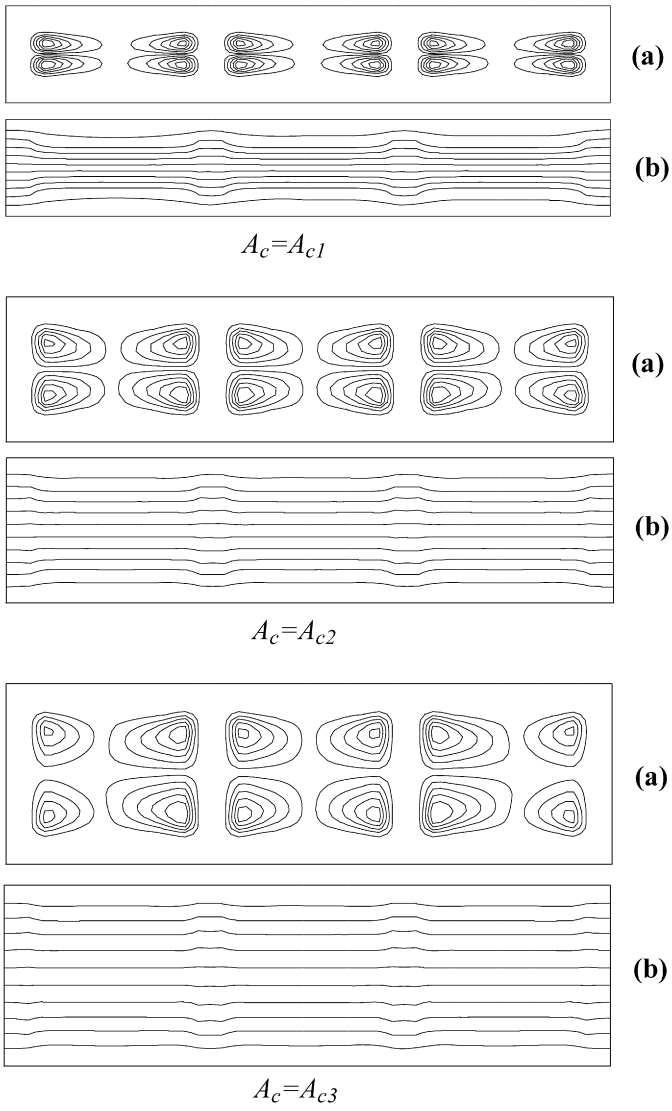

Fig. 10. Streamlines (a) and isotherms (b) obtained in heating from above for $\Delta T = 15\,^{\circ}\mathrm{C}$ and different A_c.

$$-\frac{H}{ex_3}\int_{\frac{ex_1+ex_2+2l}{H}}^{\frac{ex_1+ex_2+ex_3+2l}{H}} \left.\frac{\partial \theta_s}{\partial Y}\right|_{Y=Y_0} \mathrm{d}X$$

$$-\frac{H}{ex_4}\int_{\frac{(L-ex_4)}{H}}^{\frac{L}{H}} \left.\frac{\partial \theta_s}{\partial Y}\right|_{Y=Y_0} \mathrm{d}X$$

$$Q_{\mathrm{conv}} = -\frac{H}{l}N_k\left[\int_{\frac{ex_1}{H}}^{\frac{ex_1+l}{H}} \left.\frac{\partial \theta_f}{\partial Y}\right|_{Y=Y_0} \mathrm{d}X + \int_{\frac{ex_1+ex_2+l}{H}}^{\frac{ex_1+ex_2+2l}{H}} \left.\frac{\partial \theta_f}{\partial Y}\right|_{Y=Y_0} \mathrm{d}X\right.$$

$$\left. + \int_{\frac{L-ex_4-l}{H}}^{\frac{L-ex_4}{H}} \left.\frac{\partial \theta_f}{\partial Y}\right|_{Y=Y_0} \mathrm{d}X\right]$$

Table 4
Percentages of the contribution of each heat transfer process

ΔT (°C)	% Q_{cond}	% Q_{conv}	% Q_{rad}
5	60.93	10.89	28.18
10	59.3	12.1	28.6
20	56.1	14.6	29.3
30	51.8	16.01	32.19

Table 5
Overall thermal conductances for different type hollow blocks heated from below and from above

Aspect ratio	U'_b (W m^{-2} K^{-1})	U'_a (W m^{-2} K^{-1})
A_c=$A_{c1} \approx 1/4$	4.83	3.92
A_c=$A_{c2} \approx 1/2$	4.12	3.15
A_c=$A_{c3} \approx 1$	3.63	2.83

$$Q_{rad} = \frac{H}{l} N_r \left[\int_{\frac{ex_1}{H}}^{\frac{ex_1+l}{H}} Q_r(X)\,dX + \int_{\frac{ex_1+ex_2+l}{H}}^{\frac{ex_1+ex_2+2l}{H}} Q_r(X)\,dX + \int_{\frac{L-ex_4-l}{H}}^{\frac{L-ex_4}{H}} Q_r(X)\,dX \right]$$

Table 4 gives the contributions of the three processes in the overall heat transfer for $A_c = A_{c2} \approx 1/2$ and different values of ΔT. As expected, the conduction is predominant because it represents more than 50% of the overall heat flux Q. The contribution of the radiation heat transfer is about 30%. Finally, the convection contribution does not exceed 20% in all processed cases.

The variation of the mean heat flow crossing the hollow blocks as a function of the temperature difference ΔT had been presented in Fig. 6. This variation is practically linear in spite of the non linear character of heat transfers by convection and radiation in the inner cavities. This is due to the predominance of the conduction heat transfer shown previously.

Taking into account this pseudo-linear behavior, an overall conductance U' can be derived that permits fast and easy prediction of the overall heat transfer through the hollow structure for a given temperature difference ΔT between its upper and lower surfaces. Then, the mean heat flux Q can be expressed as:

$$Q = U'.\Delta T \tag{14}$$

where U' is the mean of the conductances $U'_i = \frac{Q_i}{\Delta T_i} (i = 1, n)$ obtained for n different values of ΔT_i. So, U' is given by:

$$U' = \frac{1}{n} \sum U'_i = \frac{1}{n} \sum_{i=1}^{n} \frac{Q_i}{\Delta T_i}$$

For each hollow block, there are two conductances corresponding to the two types of heating: heating from below (U'_b) and from above (U'_a). Table 5 gives the thermal conductances generated for the three considered types of hollow blocks. As expected, for a given hollow block, the U'_a value is very lower than the U'_b one because of the absence of natural convection in the heating from above case. The relative difference between the two values of U' is about 23.2% for $A_c \approx 1/4$ and 28.3% for $A_c \approx 1$. Also, the results obtained (Fig. 11) show that the U'_b and U'_a values decreases significantly when A_c increases in spite of the increase of the convection heat transfer rate outlined when the blocks are heated from below. This is mainly due to the diminishing of the conduction heat transfer rate when the air space in the vertical direction (y direction) increases. The reduction of the U'_b value is about 14.7% when A_c vary from 1/4 to 1/2 and about 24.8% when A_c passes from 1/4 to 1. The reduction of the U' value is more pronounced for the heating from above case. In fact, the relative change in U'_a values is about 19.6% between $A_c \approx 1/4$ and $A_c \approx 1/2$ and 27.8% between $A_c \approx 1/4$ and $A_c \approx 1$. This is due to the fact that in the heating from below cases the natural convection rate increases when A_c does and tends to homogenize the temperature distribution in the cavities inducing a reduction of the radiation heat exchanges between the inner sides of each cavity. Therefore the reduction of U'_b value when A_c increases is lower than that of U'_a.

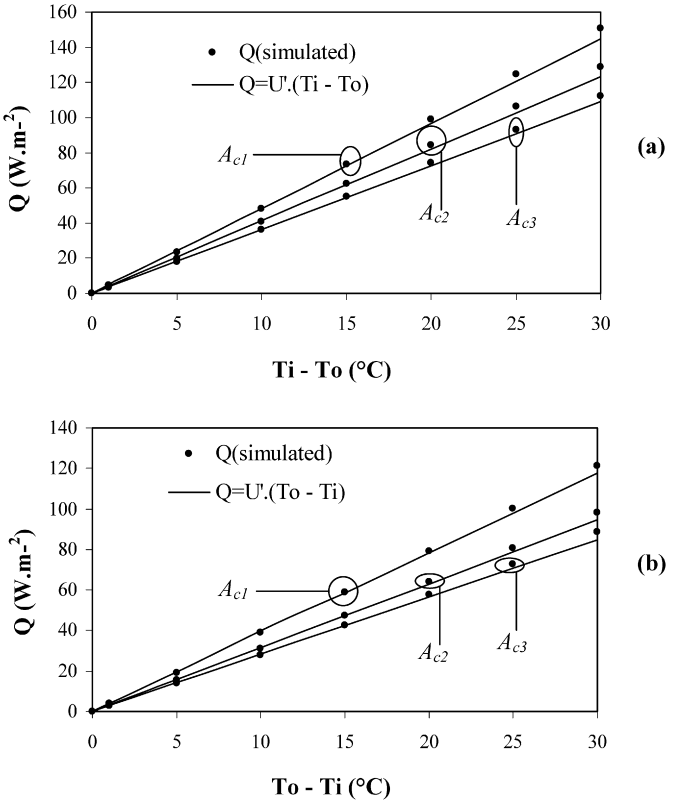

Fig. 11. Comparison of the global heat flux calculated by the code of simulation and these one predicted by the overall conductances for the structure in the cases: (a) heated from below; (b) heated from above.

3.4. Comparison of the thermal conductances U' with those obtained in the literature

The model proposed in this work is applied to predict thermal conductances given by the Scientific and Technical Center of Building (CSTB) [14]. Table 6 gives the values of U'

Table 6
Comparison of the overall thermal conductances obtained by our model with those of Ref. [14]

	Our results ($W\,m^{-2}\,K^{-1}$)		Results obtained in Ref. [14] ($W\,m^{-2}\,K^{-1}$)	
	U' ($k_s = 1.4\ W\,m^{-1}\,K^{-1}$)	U' ($k_s = 0.7\ W\,m^{-1}\,K^{-1}$)	U' ($k_s = 1.4\ W\,m^{-1}\,K^{-1}$)	U' ($k_s = 0.7\ W\,m^{-1}\,K^{-1}$)
($h = 12.4$ cm)	7.346	5.05	7.692	5.263
($h = 8.4$ cm)	8.850	6.255	9.09	6.250

for concrete hollow blocks with $k_s = 1.4\ W\,m^{-1}\,K^{-1}$, or $k_s = 0.7\ W\,m^{-1}\,K^{-1}$, $ex_i\,(i = 1\text{ to }4) = 1.8$ cm, $ey_1 = 1.8$ cm, $ey_2 = 5.8$ cm, $l = 16$ cm, $h = 12.4$ cm or $h = 8.4$ cm. It should be noted that, in Ref. [14], the effect of convection heat transfer in the heating from below case is neglected. This approximation can be justified by the results obtained in the present work which show that the effect of convection heat transfer is not much important compared to both conduction and radiation heat transfers. As it can be seen, there is a very good agreement between the results of the present work and those presented in Ref. [14]. In fact, the maximum differences induced does not exceed 4.5%.

4. Conclusion

Interactions between heat transfers by natural convection, conduction and radiation in horizontal hollow blocks, heated from below or from above, have been studied numerically. It had been shown that the thermal behavior of the block and the flow structures in the inner cavities depend strongly of the cavities aspect ratio. The variation of the overall heat flux through the hollow block as a function of the temperature difference between the horizontal sides of the block has been found to be almost linear because of the predominance of the conduction heat transfer. So, overall thermal conductances have been generated for the two types of heating (heating from below or from above). The conductances permit fast and accurate prediction of combined heat transfers through the different hollow blocks considered without solving the complex problem of the coupling between the three mechanisms of heat transfer.

References

[1] J.L. Balvanz, T.H. Kuehn, Effect of wall conduction and radiation on natural convection in a vertical slot with uniform heat generation on the heated wall, ASME HTD 8 (1980) 55–62.

[2] D.M. Kim, R. Viskanta, Study of the effects of wall conductance on natural convection in differentially oriented square cavities, J. Fluid Mech. 144 (1984) 153–176.

[3] C. Balaji, S.P. Venkateshan, Interaction of surface radiation with free convection in a square cavity, Int. J. Heat Fluid Flow 14 (1993) 260–267.

[4] C. Balaji, S.P. Venkateshan, Correlation for free convection and surface radiation in a square cavity, Int. J. Heat Fluid Flow 15 (1994) 249–251.

[5] M. Akiyama, O.P. Chong, Numerical analysis of natural convection with surface radiation in a square enclosure, Numer. Heat Transfer, Part A 31 (1997) 419–433.

[6] N. Ramesh, S.P. Venkateshan, Effect of surface radiation on natural convection in a square enclosure, J. Thermophys. Heat Transfer 13 (1999) 299–301.

[7] N. Ramesh, C. Balaji, S.P. Venkateshan, Effect of boundary conditions on natural convection in an enclosure, Int. J. Trans. Phenomena 1 (1999) 205–214.

[8] A. Abdelbaki, Z. Zrikem, Simulation numérique des transferts thermiques couplés à travers les parois alvéolaires des bâtiments, Int. J. Thermal Sci. 38 (1999) 719–730.

[9] A. Abdelbaki, Z. Zrikem, F. Haghighat, Identification of empirical transfer function coefficients for a hollow tile based on detailed models of coupled heat transfers, Building and Environment 36 (2001) 139–148.

[10] M. Hasnaoui, E. Bilgen, P. Vasseur, Natural convection heat transfer in rectangular cavities partially heated from below, J. Thermophys. Heat Transfer 6 (1992) 255–264.

[11] E.K. Lakhal, M. Hasnaoui, E. Bilgen, P. Vasseur, Convection naturelle dans une cellule carrée chauffée périodiquement par le bas: Etude numérique, Rev. Gén. Therm. Fr. 392–393 (1994) 480–485.

[12] M. Strada, J.C. Heinrich, Heat transfer rates in natural convection at high Rayleigh numbers in rectangular enclosures: A numerical study, Numer. Heat Transfer 5 (1982) 81–93.

[13] F.J. Hamady, J.R. Lloyd, H.Q. Yang, K.T. Yang, Study of local natural convection heat transfer in an inclined enclosure, Int. J. Heat Mass Transfer 32 (1989) 1697–1708.

[14] Document Technique Unifié DTU, Cahiers du Centre Scientifique et Technique du Bâtiment, CSTB, Paris 16, livraison 378, cahier 2946, "Règles de calcul des caractéristiques thermiques utiles des parois de construction". Référence AFNOR DTU P 50-702, Février 1997.